

Fig. 10. Macro photograph of specimens after 5-h exposure in Runs 6 and 7 conducted at 593°C (1100°F).

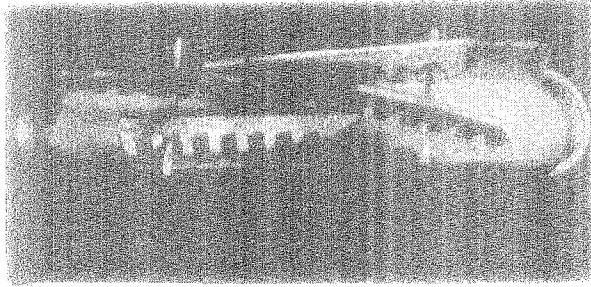
metallic specimens consisting of Fe- and Ni-base alloys, lead to $a_c \gg 1$, i.e., copious amounts of carbon deposit even after only 5 h. The results from exposures in Runs 1 through 7 also indicated that pure Fe and Fe-base alloys were more susceptible to carbon deposition and metal dusting than pure Ni and Ni-base alloys. Further, the presence of Fe- and Ni-base alloys in the same experiment led to deposit of carbon not only on Fe-base alloys but also on Ni-base alloys, indicating a cross contamination of Ni-base alloys. Therefore, additional experiments were performed in which the Fe- and Ni-base alloys were exposed separately to avoid cross contamination and to assess their inherent behavior in the metal dusting environment.

To examine the role of catalytic effect on gas phase reactions, Runs 8 and 9 were conducted in the same gas environment with high purity alumina specimens and without any metallic specimens. After 75 h exposure at 593°C (1100°F) in Gas 4 and 5, virtually no carbon was detected on the alumina specimens (see Fig. 11). These results indicate that a viable catalytic material is essential to establishing high carbon activity and associated deposition of carbon. This experiment also indicates that coatings, such as alumina, may offer protection against carbon deposition and subsequent metal dusting of certain metallic structural materials.

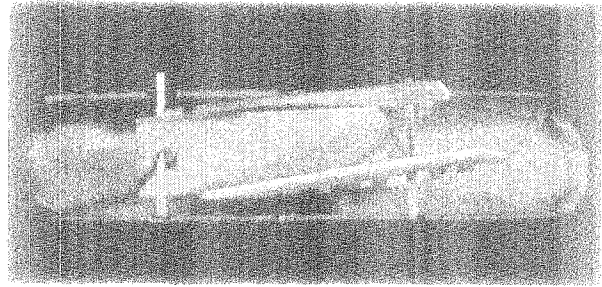
Run 10 was conducted for 90 d in one of three new systems under the same conditions as in Run 2 to validate the adequacy of the new equipment and reproducibility of the results.

Characteristics of Carbon Deposits

Scanning electron microscopy (SEM), Raman spectroscopy, and X-ray diffraction (XRD) analyses have been used to study the microstructure, electron binding, and phase chemistry of the metal dusting products. Thus far, the investigations have focused on defects in the metals. Defects in the carbon dust have hardly been studied, even though carbon is an integral part of the metal dusting process. Graphite has a layered



Run 8



Run 9



Fig. 11. Macrophotograph of specimens after 72-h exposure in Runs 8 and 9 conducted at 593°C (1100°F).

structure with the space group $P6_3/mmc$ (see Fig. 12). Carbon atoms within the layers bond strongly through sp^2 hybridization and arrange in a two-dimensional honeycomb network. The layers are stacked in a hexagonal crystal structure and are bound together by van der Waals force. Because the van der Waals force is weak, the C-C distance between layers is large (335.4 pm).¹¹ For this reason, graphite crystals readily disorder along the c-axis.¹²

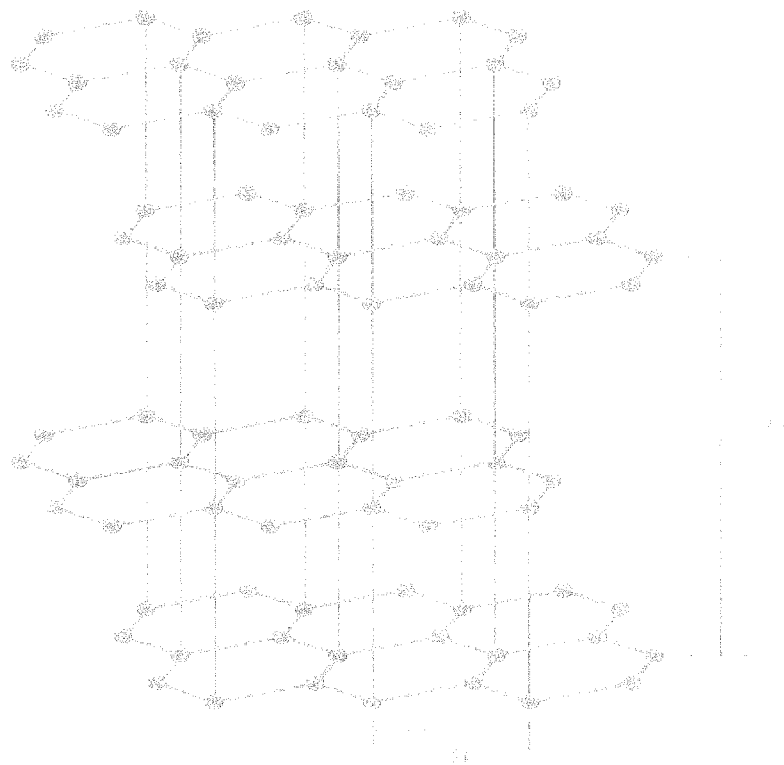


Fig. 12. Structure of graphite. Carbon atoms within layers arrange in two-dimensional honeycomb network; layers are stacked in a hexagonal crystal structure.

The Raman scattering from various forms of carbon is sensitive to the structural disorder of the material.¹³⁻¹⁶ As a result, Raman spectroscopy provides a useful nondestructive technique for structural characterization of carbon materials. Lattice defects in graphite break down the hexagonal symmetry of the graphite lattice and modify the optical selection rules for the lattice vibrational modes that are observable in Raman scattering. A single Raman line, the E_{2g2} vibration mode, is theoretically expected for the hexagonal lattice of graphite and has been observed at 1575 cm^{-1} in natural graphite. In glassy carbon, the layers are parallel, but their mutual orientation is random in the direction of the planes (due to the weak link between the layers). A band at 1355 cm^{-1} observed for glassy carbon has been assigned to a defect-activated vibrational mode originating from the distorted hexagonal lattice of graphite near the crystal boundary. The two bands at 1355 and 1575 cm^{-1} are designated as D (distorted) and G (graphite), respectively. The relative intensity ratio I_D/I_G and the relative bandwidths increase in progression from single-crystal graphite through polycrystalline graphite up to glassy carbon; hence, these values can be used as a measure of imperfection of the graphite layer planes.¹³⁻¹⁶ These parameters are more defect sensitive than are the XRD parameters that define crystalline size. Therefore, Raman spectroscopy represents a useful tool for investigating the defects in carbon structures and their relationship to the metal dusting phenomenon.

Raman spectroscopy measurements were made for carbon deposited on pure Fe specimens during exposure in different experiments. The Spectra were obtained with a Renishaw System 2000 imaging Raman microscope equipped with a He-Ne laser that delivered $\approx 5\text{ mW}$ to the specimen. The spectra were recorded at wavelengths between 190 and 4000 cm^{-1} , with the laser partially defocused to a diameter of $\approx 5\text{ }\mu\text{m}$ to avoid burning or otherwise transforming the carbon deposits. Spectra were taken at three to six locations on a given specimen to verify that the observed surface deposits were uniform in composition. Magnetization of samples was measured by a vibrational-sample magnetometer under 1 Tesla in an argon atmosphere.

Figure 13 shows the Raman spectra (frequency range 190 - 1000 cm^{-1} , 1000 - 2000 cm^{-1} , and 2000 - 4000 cm^{-1}) of carbon "soot" from Runs 4, 5, and 7 along with Raman spectra of polycrystalline graphite and pencil "lead." It is evident that the two bands at 1355 and 1575 cm^{-1} are similar, but the carbon from the metal dusting runs exhibits broader peaks than the graphite block and pencil lead. Figure 14 shows the XRD pattern for the coke and carbon layer on the iron sample.

The major phases in the metal dusting product are graphite and Fe_3C . There may be a small amount of Fe_3O_4 , which presents a weak diffraction peak at $2\theta = 35.4^\circ$. According to the mechanism proposed by Hochman,⁴ Fe_3C decomposes to Fe and C at

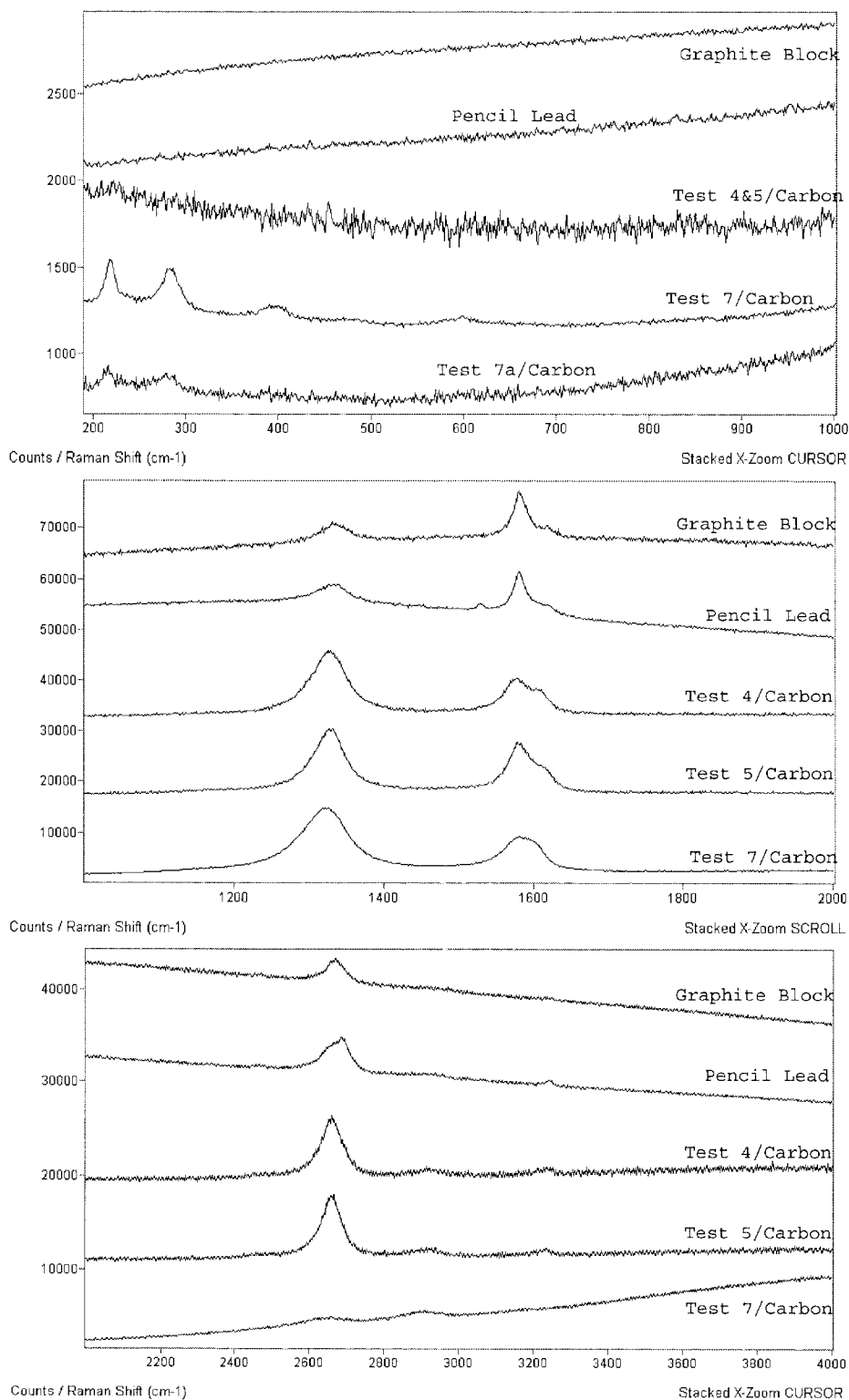


Fig. 13. Raman spectra (frequency range 190-1000 cm^{-1} , 1000-2000 cm^{-1} , and 2000-4000 cm^{-1}) of carbon "soot" from Runs 4, 5, and 7 along with Raman spectra of polycrystalline graphite and pencil "lead." Tests 4 and 5 were run for 100 h at 1300°F and Test 7 was run for 5 h at 593°C (1100°F).

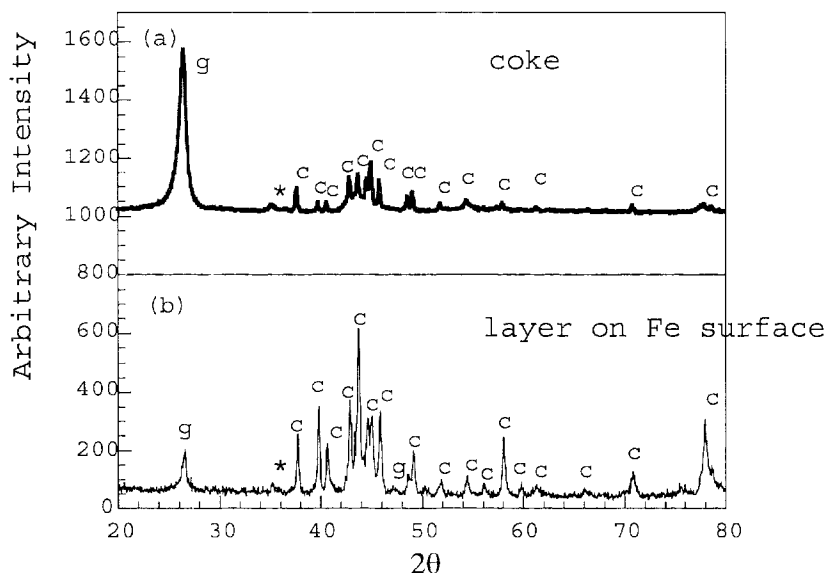


Fig. 14. XRD pattern of coke and surface layer on iron sample after exposure to Gas 4 at 593°C (1100°F) for 100 h. Major phases are graphite (g) and cementite (c); there may be a small amount of Fe₃O₄, whose strongest peak is indicated by *.

the final step, in which case the final products should be Fe and C. However, no iron diffraction peak appears in the metal dusting product. XRD may not be able to detect the phase if the concentration is <5%. Therefore, a magnetic measurement method was used to determine if iron was present. Iron is a strong ferromagnetic material with Curie temperature (T_c) at 770°C.¹⁷ A huge magnetization increase would be observed at 770°C, if there was evidence of iron in the metal dusting product. Figure 15 shows the magnetization of the metal dusting product as a function of temperature. The large transition of magnetization at 210°C is due to Fe₃C.¹⁷ The small magnetization increase at 582°C may be due to small amount of ferromagnetic Fe₃O₄ with T_c at 585°C. However, there is no obvious transition of magnetization around 770°C. The very small magnetic moment around 700°C indicates that the concentration of regular α -iron in the product of metal dusting is below 0.1%. It is possible that XRD and magnetic measurement cannot detect some iron particles with very small size. However, both XRD and magnetic measurement show that the major phase in coke is Fe₃C, not Fe phase. Fe₃C is the final product of metal dusting instead of only the intermediate compound surmised by Hochman's mechanism.⁴ Therefore, further investigation is needed to establish the causes of metal dusting and methods to mitigate it under our experimental conditions.

The XRD [002] peak widths of the carbon dust are broader than those of the well-crystallized graphite (Fig. 16). We interpret this observation as indicating that the crystallinity of carbon dust is poorer than that of graphite. However, the [002] peak

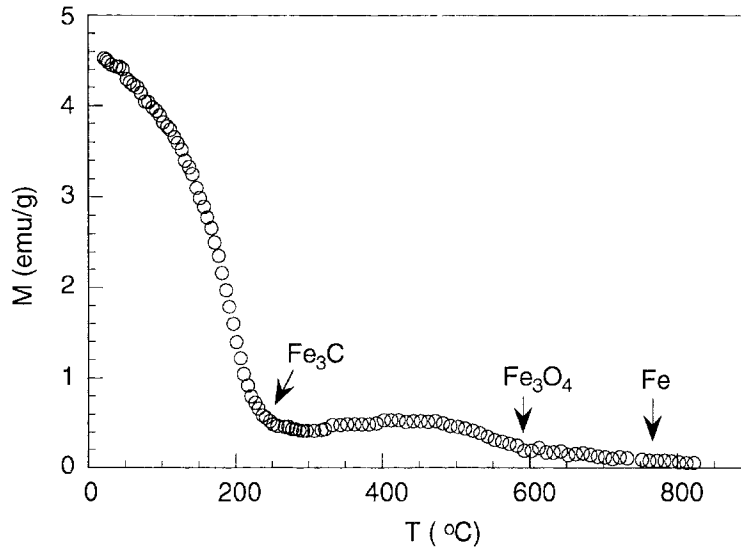


Fig. 15. Temperature dependence of magnetization (M) of metal dusting product obtained in Run 4 at 593°C (1100°F).

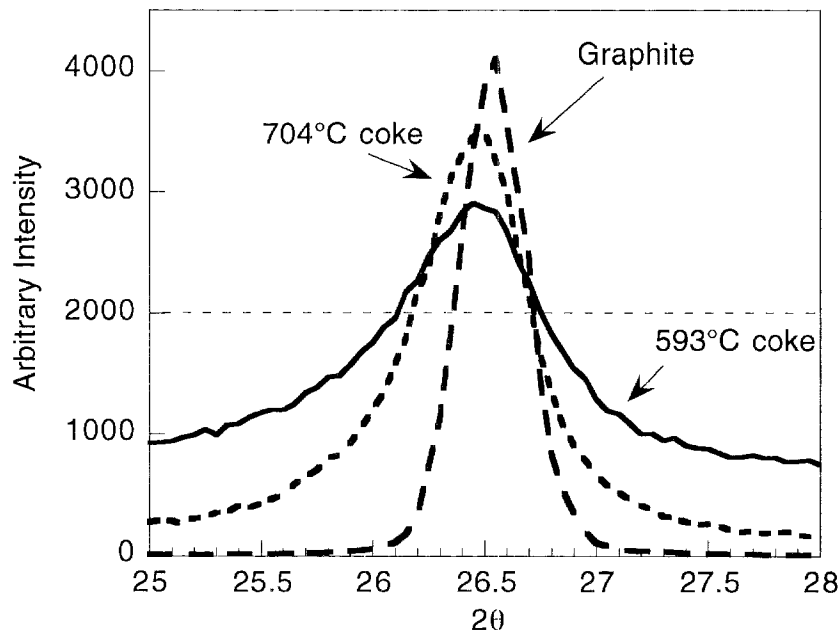


Fig. 16. Peak widths of [002] diffraction from graphite and coke (at 593 and 704°C). Narrower peak width indicates better crystallinity.

widths of the coke are much narrower than that of glassy carbon (see Fig. 17). Table 5 shows that the coke crystallite sizes are much larger than those of glassy carbon. The coke crystallite sizes are also considerably larger than those reported for other carbonaceous materials made at a similar temperature.¹⁸⁻²⁰ The interlayer distances of the carbon plane are related to the degree of disorder. The layers are not parallel in the disoriented graphite structure. Average interlayer plane distance increases when the layers are disoriented. The interlayer plane distance is 3.354 Å for single-crystal

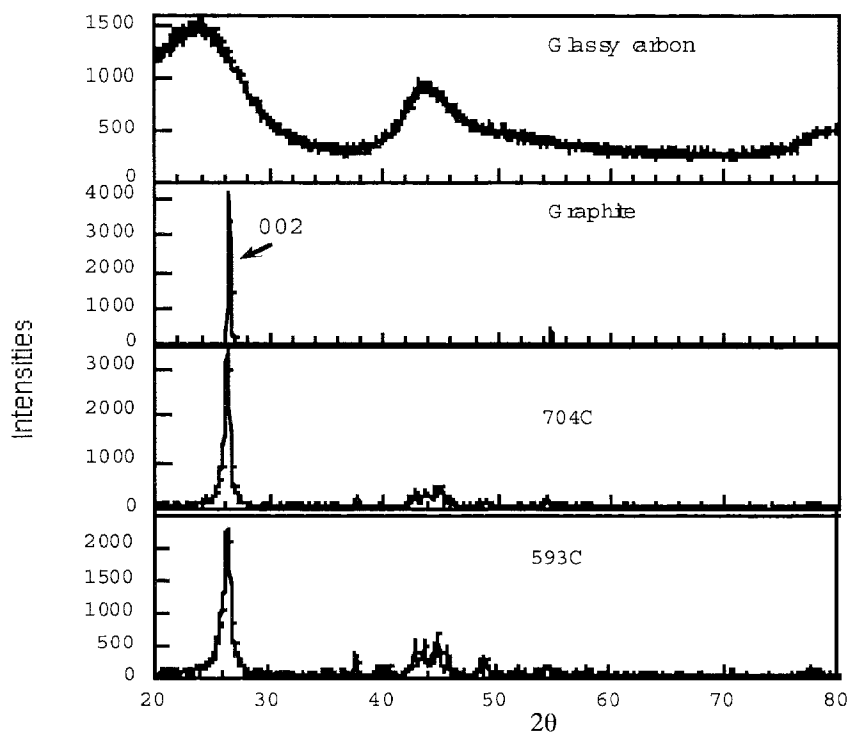


Fig. 17. Peak widths of [002] diffraction from glassy carbon, graphite, and coke (593 and 704°C). Narrower peak width indicates better crystallinity.

Table 5. Crystallite dimension and interlayer plane distance of graphite, coke (593 and 704°C), and glassy carbon. Δ is difference of interlayer plane distance of carbon from single-crystal graphite (with interlayer plane distance 3.354 Å).

	Interlayer plane distance (Å)	Δ (Å)	Crystallite size (Å)		Mean number of layers per particle
			c-axis	a-axis	
Graphite	3.356	0.002	220	299	65.7
Coke developed at 704°C	3.362	0.006	145	151	43.3
Coke developed at 593°C	3.365	0.011	110	127	32.8
Glassy carbon	3.736	0.382	12	15	3.4

graphite.¹¹ The interlayer plane distance of coke is very close to that of the well-crystallized graphite. Franklin¹¹ proposed the following relationship for the proportion of disoriented layer (p) as a function of interlayer plane distance (d):

$$d = 3.44 - 0.086(1 - p^2).$$

According to this relationship, the interlayer plane distances of coke made at 704°C, 3.362 Å (Table 5), indicates carbon having $\approx 70\%$ three-dimensional ordering. For the carbons produced by conventional treatment of carbon-containing raw materials, $>2000^\circ\text{C}$ is required for thermal recrystallization to occur and to obtain this high degree of three-dimensional ordering.^{18,19}

Raman spectra of coke, glassy carbon, and graphite are presented in Fig. 18. The well-crystallized graphite shows two peaks: the sharp band at 1580 cm^{-1} (G band) can be assigned to the E_{2g} C-C stretching mode.²¹⁻²³ The other peak, at 2685 cm^{-1} , is a two-phonon band taken to be $2 \times 1330\text{ cm}^{-1}$. The first-order phonon band at 1330 cm^{-1} (D band) is not observed for well-crystallized graphite because of the $k = 0$ selection rule.²¹ However, disorder in the lattice can cause a breakdown of this selection rule, which is why the 1330 cm^{-1} band is observed in the Raman spectra of glassy carbon. Symmetry

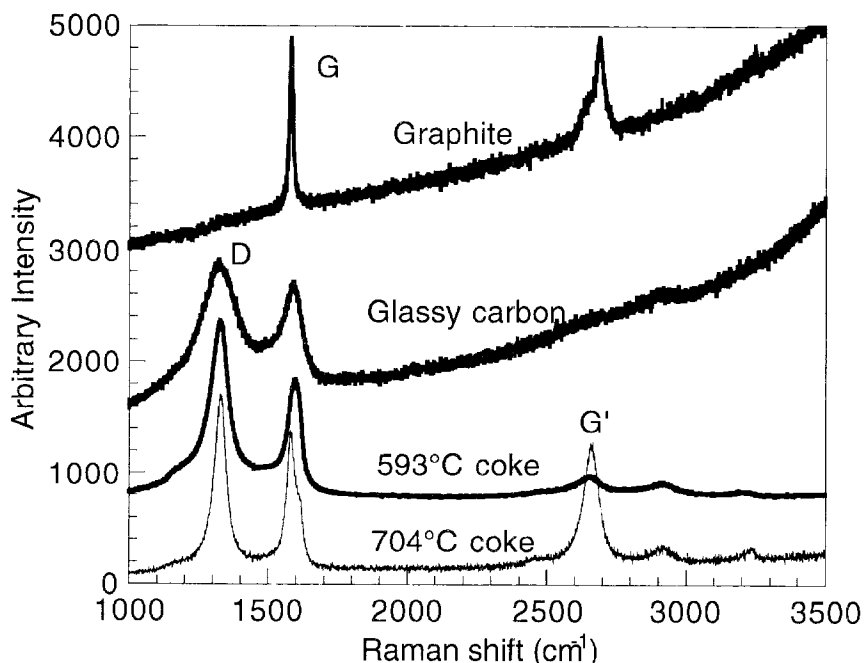


Fig. 18. Raman spectra of graphite, glassy carbon, and coke made at 593°C and 704°C. The 1330 cm^{-1} band is designated as D because its character is related to disorder of the graphite phase, whereas the 1580 and 2680 cm^{-1} bands are assigned to G and G', respectively.

may also be affected by a high degree of disorder that could, for example, cause the second-order phonon at 2685 cm^{-1} to disappear in the Raman spectra of glassy carbon. The 2685 cm^{-1} band is designated as G' because its character is similar to that of the G band. The highly disordered carbons have very broad Raman bands, and the intensity of the 1330 cm^{-1} band increases when carbon becomes more disordered. The intensities of the D band are considered to depend on the in-plane displacements, which lead to a loss of hexagonal symmetry in the two-dimensional lattice within the graphite planes.²² A shoulder at 1617 cm^{-1} in the cokes formed at 704°C is also

dependent on structural disorder and is, therefore, designated as the D' band (Fig. 19). Its behavior is qualitatively similar to that of the D band.^{24,25} The 2920 cm⁻¹ peak for the 704°C coke arises from a combination of the strong density of states at ~1330 and 1617 cm⁻¹.²⁶ The 3235 cm⁻¹ band is the first overtone of the G band.²²

The widths of the Raman bands for the coke from the dusting process are between those of well-crystallized graphite and glassy carbon. The D/G intensity ratio of coke made at 704°C is lower than that of coke made at 593°C, and the D band for coke made at 704°C is obviously narrower (see Fig. 19). The G band at 1583 cm⁻¹ and the D' band at 1617 cm⁻¹ separate in the coke made at 704°C, whereas the G and D' bands of the coke made at 593°C remain merged in one broad band. The bandwidths and the D/G intensity ratio are related to the crystallinity of the carbon dust.¹³⁻¹⁶ Therefore, the coke made at 704°C is better crystallized than the coke made at 593°C. The intensity of the G' band at 2685 cm⁻¹ is reported to be highly sensitive to the structure.²⁷ For the coke made at 704°C, the G' band is much stronger than for coke made at 593°C, and the G' bandwidth (71 cm⁻¹ at half height) of the coke made at 704°C is narrower than the G' bandwidth (112 cm⁻¹ at half height) of coke made at 593°C. This finding also indicates that the coke made at 704°C is better crystallized than that made at 593°C.

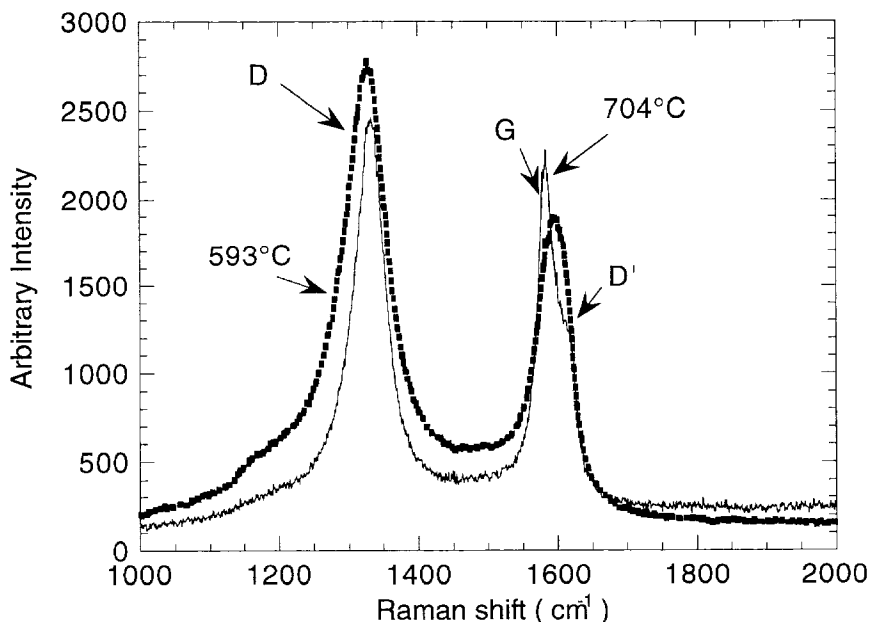


Fig. 19. Raman spectra of coke made at 593°C and 704°C. Raman bandwidth for coke made at 704°C is narrower than that for coke made at 593°C. D/G intensity ratio for coke made at 593°C is 1.5, whereas that for coke made at 704°C is only 1.1.

As mentioned earlier, a layer of carbon closely adheres to the surface of the tested alloys. The Raman spectra in Fig. 20 show that the Raman band for the carbon on the surface of the iron has a narrower width than that for coke at some distance from the surface. This finding may indicate that carbon in the tightly adhering layer of the iron

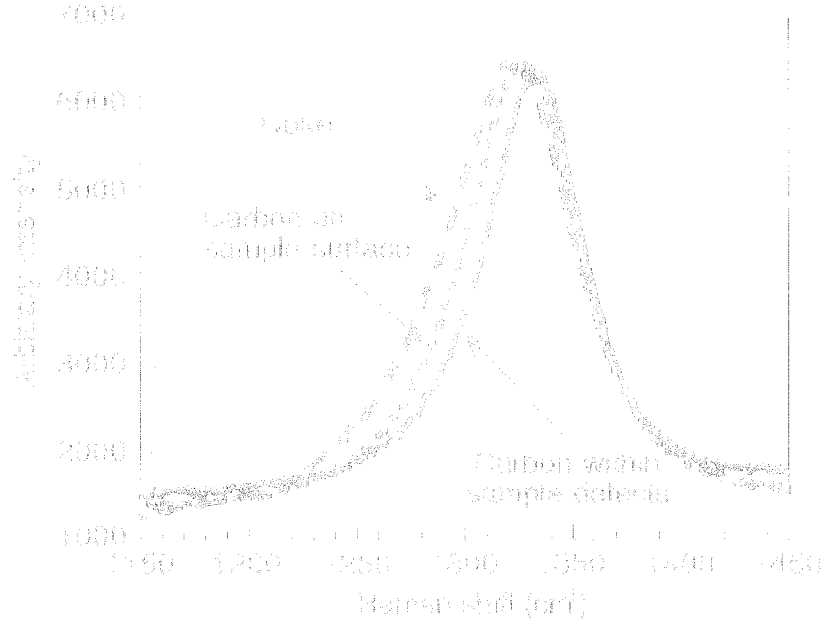


Fig. 20. EDS spectra of color, carbon on alloy sample surface, and carbon in sample volume.

surface had better crystallinity. The SEM cross section of the Fe-Al alloy (Fig. 21), indicates the effect of porosity in the material on carbon deposition and initial oxidation. Carbonaceous gases diffused and precipitated inside the alloy. EDS analysis revealed that the dark areas are filled with carbon. EDS spectra were obtained by scanning the laser on the carbon deposits in the Fe-Al coating by-



Fig. 21. SEM cross section of Fe-Al alloy after metal coating experiment at 1400°C (1100°F). Carbon has diffused into and precipitated within the alloy. Energy dispersive X-ray spectroscopy (EDX) indicated that the dark areas are filled with carbon.

Figure 20 shows that the line width of the Raman band for the carbon in the alloy defects is narrower than that for the coke and the surface carbon. The band position is shifted slightly to a higher frequency (10 cm^{-1}) for the carbon in iron. Therefore, the crystallinity of carbon increases progressively from coke through surface carbon to the carbon within the metal after metal dusting.

Proposed Metal Dusting Mechanism

The experimental results from Raman, XRD, and SEM measurements shed some light on the mechanism of metal dusting. There appears to be a relationship between metal dusting and degree of crystallization of the carbon dust. Our interpretation of the crystallizing process for carbon during dusting is shown in Fig. 22. In the initial stage, single carbon atoms are deposited on the surface of the iron; they then either dissolve in the iron or accumulate to form small carbon particles. There are dangling bonds on the surface and many defects, such as vacancies and distorted bonds in the small particles. All of these surface and internal defects increase the free energy of these particles compared to that of well-crystallized graphite. At higher temperature, where the carbon atoms have enough energy to migrate, the carbon recrystallizes from small-distorted particles to large well-crystallized graphite. However, because the C-C bond is very strong (the melting temperature of carbon is 4492°C), the recrystallization process requires a higher temperature. Achieving good crystallinity with carbon below 1000°C is problematic for the following reasons. First, the carbon layers in graphite structure are easily disoriented because the van der Waals forces between the layers are very weak. Second, recrystallization below 1000°C is hindered because the bond in the layers is too strong.

The catalysts such as iron or cementite could dramatically increase the rate of carbon recrystallization (right column in Fig. 22). The cementite structure has been described as a framework of almost close-packed iron atoms held together by metallic bonding to the small carbon atoms in the largest interstices. Carbon occupies only one-sixth of the interstices, allowing carbon to dissolve in and move through those interstices. When carbon dissolves in the iron or cementite, the Fe-C bond is much weaker than the C-C bond, and transportation of carbon atoms is greatly facilitated. Therefore, the poorly crystallized coke can transfer through iron and eventually achieve improved crystallinity. Reducing the number of dangling bonds on the surface and the number of internal defects in the carbon particles reduces the free energy.

Figure 23 shows the catalytic recrystallization process. Carbon atoms are deposited on the surface of Fe_3C . As mentioned above, the carbon layers in the graphite structure are easily disoriented because the van der Waals forces between the layers are weak. Carbon can not grow with good crystallinity if the lattice planes of Fe_3C do not match the graphite lattice planes to help the crystallization of carbon (upper part in Fig. 23). When

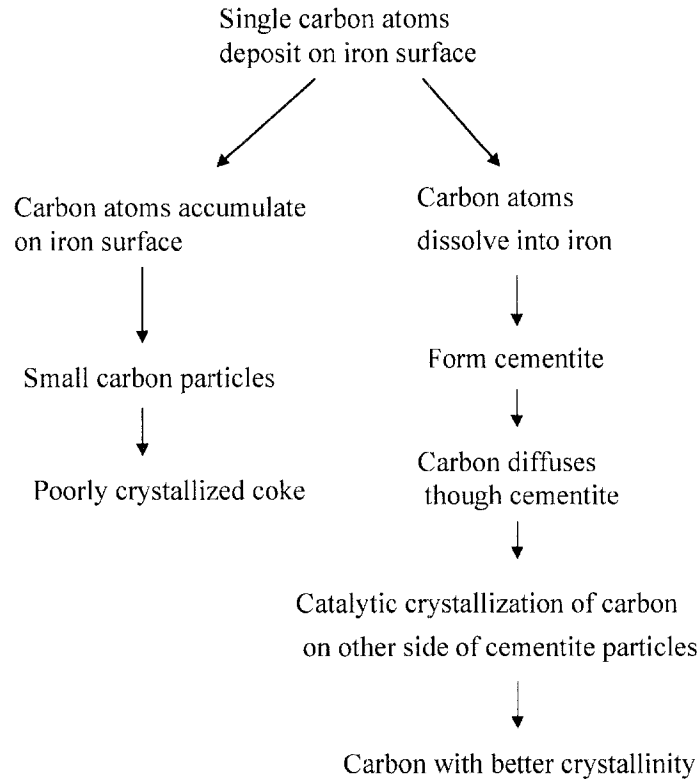


Fig. 22. Proposed process for carbon crystallization after deposition in metal-dusting environment.

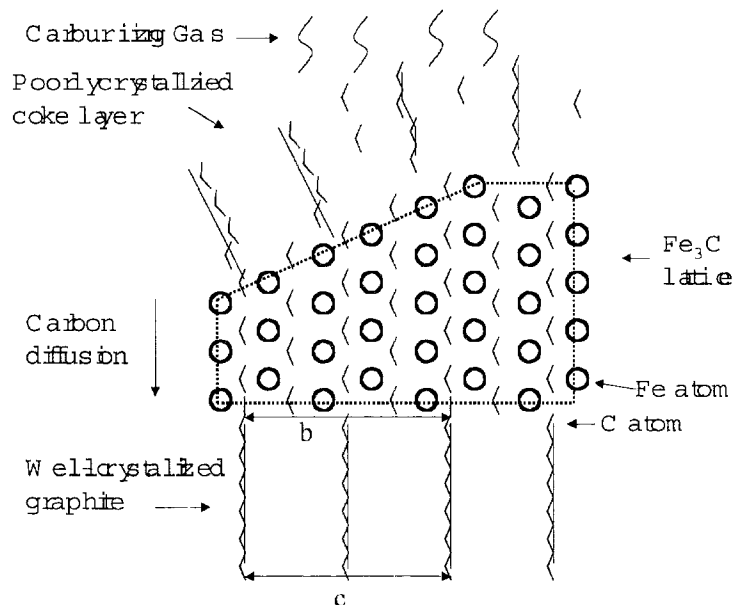


Fig. 23. Proposed process for catalytic crystallization. Poorly crystallized carbon dissolves in and diffuses through cementite, whose lattice provides excellent orientation for crystallization of graphite; b dimension of cementite (6.743 \AA) is very close to c dimension of graphite (6.724 \AA).